Compositional dependence of the magnetic properties of epitaxial FeV/MgO thin films

T. Devolder, T. Tahmasebi, S. Eimer, Thomas Hauet, Stéphane Andrieu

Compositional dependence of the magnetic properties of epitaxial FeV/MgO thin films

T. Devolder, T. Tahmasebi, S. Eimer, T. Hauet, and S. Andrieu

Citation: Applied Physics Letters **103**, 242410 (2013); doi: 10.1063/1.4845375
View online: http://dx.doi.org/10.1063/1.4845375
View Table of Contents: http://scitation.aip.org/content/aip/journal/apl/103/24?ver=pdfcov
Published by the AIP Publishing

Compositional dependence of the magnetic properties of epitaxial FeV/MgO thin films

T. Devolder,[1,2,a)] T. Tahmasebi,[3] S. Eimer,[1,2] T. Hauet,[4] and S. Andrieu[4]
[1]*Institut d'Electronique Fondamentale, CNRS, UMR 8622, Orsay, France*
[2]*Univ. Paris-Sud, 91405 Orsay, France*
[3]*IMEC, Kapeldreef 75, B-3001 Leuven, Belgium*
[4]*Institut Jean Lamour, CNRS - Universite de Lorraine, Boulevard des aiguillettes BP 70239, F-54506 Vandoeuvre le's Nancy, France*

(Received 2 August 2013; accepted 23 November 2013; published online 11 December 2013)

Owing to their bcc structures and the low lattice misfit with MgO, FeV alloys are interesting for MgO-based magnetic tunnel junctions. We use vector network analyzer ferromagnetic resonance to measure the magnetization, anisotropy, exchange stiffness, and damping of epitaxial FeV/MgO thin alloys of various V contents. The low magnetization, very high exchange stiffness (23 pJ/m) and very low effective damping (<0.0026) of the alloy with 20% V content makes it an interesting candidate for spin torque applications. The ultralow damping is consistent with a spin-orbit origin, which sheds light on the possible strategies to reduce the damping in alloys. © *2013 AIP Publishing LLC*. [http://dx.doi.org/10.1063/1.4845375]

Magnetic tunnel junctions form the base element of many spintronic devices. One of the most emblematic application is the spin-torque operated magnetic random access memory,[1] that is presently undergoing a shift from in-plane magnetized systems[2] to out-of-plane magnetized systems.[3] In this emerging "perpendicular" technology, the storage layer needs to warrant a high tunnel magneto resistance (TMR) ratio, a sufficient perpendicular anisotropy, and a low switching current. This requires to be able to crystallize the storage layer into a body-centered cubic (bcc) structure with a (001) texture, and a reasonably good lattice matching with MgO. In addition, the storage layer material also needs to have a large interface anisotropy with MgO and a low Gilbert damping. As a result, CoFeB alloys are usually chosen,[3–5] because they have the relevant properties.[6,7] However intermetallics with greater exchange stiffness and Curie temperature, together with lower magnetization M_s and lower damping are desirable. This is first to fully benefit from the interface anisotropy without paying the destabilization cost of the perpendicular demagnetizing field and second, to favor coherent magnetization reversal compared to domain wall mediated reversal.[8]

Most of the research activity has been focused on the alloying of Fe, with the aim of starting from a bcc structure and a damping much lower than Co and Ni.[9] Prior trials to add Cr, V, or Ni dopants in FeCo or FeNi systems[10,11] were found to degrade substantially either the damping factors or the TMR ratios. One thus still needs to find a material, or a material combination yielding together large TMR, low damping and low magnetization.

To find one, our reasoning is the following. Reducing the magnetization can be done by substituting iron by other transition metal elements, following the Slater-Pauling rule. To avoid miscibility problems, we should preferentially substitute with materials ordering in a bcc state (V, Cr, Mn, Nb, Mo, Ta, W) when being elemental solids, or making solid solutions with bcc Fe on the Fe-rich side. This excludes the noble metals (Au, Cu, Ag) and Ni. Our second guiding line is the search for lower Gilbert damping parameters α. Unfortunately, α is one of the last few features that cannot be calculated reliably in transition metal alloys. However, α is known[12,13] to vary like the square of the spin-orbit constant ξ^2 provided that the band structure and the Fermi level are unchanged.[14] Within a transition series, the spin-orbit constant varies[15] like Z^2, and from one transition series to the next it increases substantially.[16] A direct consequence is that one should avoid substituting iron with elements from the 4d and 5d series, and from the end of the 3d series. We are thus left essentially with V, Cr, and Mn. Mn can be excluded since it gets oxidized when in proximity with MgO,[17] which leads to poor magnetic properties. Being the lightest element, Vanadium is the best candidate for an effective reduction of the magnetization, together with a decrease of the damping.[13] Another uncommon[18,19] fact that is often forgotten is that the Curie temperature of FeV alloys increases with the Vanadium doping.[20,21] The Curie temperature is maximum for a Vanadium content of 20%. At that composition, the exchange integral between Fe atoms was predicted to be twice the value of pure iron,[20] which should favor a more coherent magnetization reversal. Another advantage of FeV alloys compared to CoFe is their small misfit with the MgO lattice. This was shown to reduce the density of misfit dislocations in the MgO barrier,[22] with a significantly increase of the TMR ratio.[23] Finally, perpendicular magnetic anisotropy[24] with some electric field tunability[25] was obtained formerly in Fe/V systems which led us to the conclusion that the potential FeV alloys deserve to be assessed.

We have prepared MgO (single-crystalline substrate)/$Fe_{1-x}V_x$ (9–30 nm)/Au (6 nm) films, with $60\% \geq x \geq 0\%$ by molecular beam epitaxy. Separate V and Fe layers of adequate thicknesses are first grown at room temperature in epitaxy with the MgO, as checked by RHEED patterns.[22] This is followed by an 800 °C annealing, which yields an efficient mixing of Fe and V, attested by the symmetry of the (002) X-ray diffraction peak (not shown). The $Fe_{1-x}V_x$ layers have bcc

a)thibaut.devolder@u-psud.fr

structure with their [100] directions rotated by 45° with respect to the MgO cubic axes. The V contents x were checked by the modeling of X-ray photoelectron spectra at the 2p lines of Fe and V, as detailed in Ref. 23. The contents were found to be consistent with the lattice spacing of the alloy as deduced from X-ray diffraction. The film thicknesses t were checked by the modeling of Grazing X-ray Reflectometry spectra. An addition series of samples has been grown by direct sputtering at room temperature from a target of the composition $Fe_{75}V_{25}$. No annealing was applied to this sample.

The determination of the magnetic properties was essentially done by Vibrating Sample Magnetometry (VSM), by Polar Magneto-Optical Kerr Effect (PMOKE), and by Vector Network Analyzer FerroMagnetic Resonance (VNA-FMR (Ref. 26)) at room temperature.

VSM loops (not shown) have confirmed that the easy axes of the cubic anisotropy were the [100] directions of FeV except for V contents of 40% and above, whose easy axes are [110]. PMOKE loops (inset of Fig. 1) were used to estimate the saturation field H_{sat} and the initial susceptibility $H_{ini} = M_S \frac{dM_z}{dH_z}$ in perpendicular fields. For a uniform sample with cubic axes $\langle 100 \rangle$, they would be $H_{sat} = M_S - H_{kc}$ and $H_{ini} = M_S + H_{kc}$, where M_S is the magnetization and H_{kc} the anisotropy field. In principle, these two quantities can be used to deduce M_S and H_{kc} and compare with the VNAFMR outcomes. For the $Fe_{50}V_{50}$ and $Fe_{58}V_{42}$ compositions only a faint similarity has been seen, which is an indication of inhomogeneous magnetic properties.

To quantify the magnetic properties, we have used VNAFMR to obtain the sample's high-frequency (1 to 70 GHz) transverse susceptibility χ_t (Fig. 1). We use the open-circuit total reflection configuration[27] with an applied field $\mu_0 H_z$ of 0–2.5 T perpendicular to the sample surface. To deduce the complex permeability μ_{eff} of the effective medium surrounding the stripline, we need a reference spectrum with vanishing susceptibility, which was obtained in zero field when the magnetization lies along the RF field radiated by the stripline. While for ultrathin films the sample transverse susceptibility χ_t is strictly[6] proportional to the μ_{eff}, this is not the case for thick metallic films because eddy current screening in the film mixes the real and imaginary parts of the sample permeability in a frequency dependent manner.[28] For small FMR linewidths, the recovery of a physical χ_t can be done by projecting $\Re(\mu_{eff})$ and $\Im(\mu_{eff})$ on symmetric and antisymmetric Lorentzian functions as examplified in Figure 1.

To analyze the characteristic features in the susceptibility spectra, we consider films with cubic anisotropy and easy axis in the film plane. The in-phase susceptibility $\Re(\chi_t)$ vanishes at the ferromagnetic resonance frequency $\omega_{FMR}/(2\pi)$. For fields $|H_z| \geq H_{sat}$, i.e., saturating the magnetization along z, we have $\omega_{FMR} = \gamma_0(|H_z| - M_S + H_{kc})$, where γ_0 is the gyromagnetic ratio. χ_t also vanishes at the frequencies of the perpendicular standing spin waves (PSSW) when the phase difference between dynamic magnetizations at the top and bottom surfaces is $n\pi$. For fields $H_z \geq H_{sat}$ and in the absence of surface pinning, this happens at frequencies

$$\omega_{PSSW} = \omega_{FMR} + \gamma_0 \frac{2A\pi^2 n^2}{\mu_0 M_s t^2}, \quad (1)$$

where A is the exchange stiffness and n the mode index which is an integer in the case of pinning-free surfaces. Unfortunately the $n \geq 3$ PSSW modes are probably too high in frequency to be observed with our technique (Fig. 2(c)). Linear fits of either ω_{FMR} or ω_{PSSW} versus H_z for fields above H_{sat} are used to get γ_0, which is then translated in a spectroscopic splitting factor g. The zero-field intercept of the curve is then used to deduce M_S–H_{kc}. The film resonance frequency at remanence is $\gamma_0\sqrt{H_k(M_S + H_{kc})}$. Its knowledge, combined

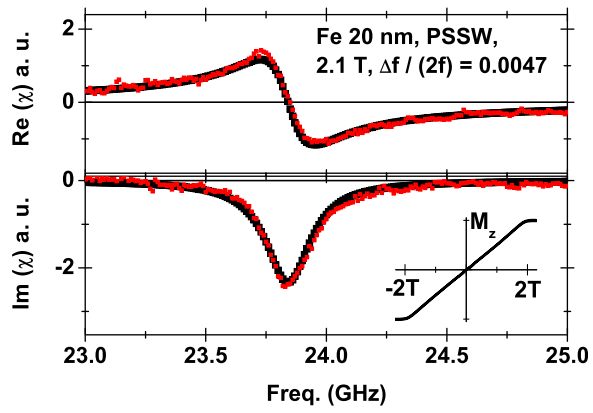

FIG. 1. Permeability spectrum recorded on a Fe(20 nm)/MgO film at an applied field of 2.1 T (red dots) perpendicular to the sample. The frequency interval is chosen to display the first ($n = 1$) perpendicular standing spin wave mode. The fit (bold black line) is done with an effective linewidth parameter $\Delta\omega/(2\omega) = 0.0047$, which includes an unknown inhomogeneous broadening contribution. Inset: PMOKE loop showing M_z versus $\mu_0 H_z$ for the same film.

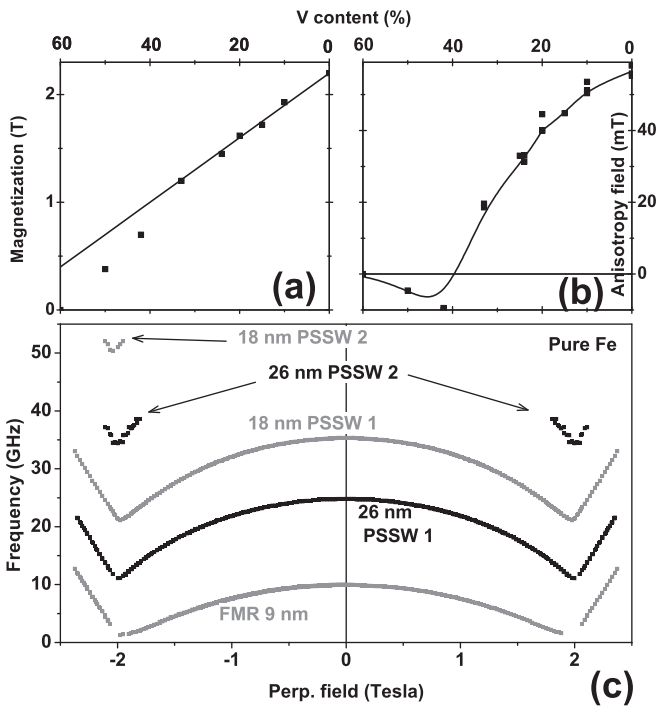

FIG. 2. (A) Magnetization versus Fe content. The dotted line is the Slater-Pauling rule. (B) Anisotropy versus Fe content. The line is a guide to the eye. (C) Field dependence of the FerroMagnetic Resonance frequencies and the perpendicular standing spin wave frequencies of Fe/MgO films of various thicknesses.

with H_{sat}, yields the magnetization M_S and the anisotropy field H_{kc}. Finally, $\omega_{PSSW} - \omega_{FMR}$ is used to deduce the exchange stiffness A. When several PSSW modes were detectable, the n^2 dependence of Eq. (1) was not observed, indicating some surface pinning of the magnetization, probably related to surface anisotropy. Because the influence of surface pinning on the spin wave wavelength increases with n, we have chosen to use only the $n=1$ mode to deduce the exchange stiffness A. The validity of this approach is yet to be clarified.

To extract the damping, we only use the high field, i.e., $|H_z| \geq H_{sat}$ data. Indeed, when the magnetization is saturated along z, two-magnon scattering is forbidden,[29] such that the FMR linewidth is only influenced by Gilbert damping α and long-range inhomogeneities of the internal field (so-called inhomogeneous broadening). The positive peak to negative peak frequency spacing of $\Re(\mu_t)$, or equivalently the full width at half maximum of the peak of $\Im(\mu_t)$ is $\Delta\omega = 2\alpha\omega_{FMR}$. Each line can thus provide an upper bound for α, and the frequency dependence of the linewidth (Fig. 3(a)) is an indication of the inhomogeneity of the internal field in the material. Note that for the $Fe_{50}V_{50}$ composition an extreme broadening was observed, as two clearly distinct FMR lines were seen (Fig. 3(b)). We report here only the results for the most intense line. The weakest mode corresponds to a region in the sample where the magnetization is reduced by 13 mT.

The magnetic properties of our films are gathered in Table I. The Landé factors are scattered in the interval $2.06 \leq g \leq 2.10$ which is essentially our error bar; they thus stay near that of pure iron ($g=2.09$). The magnetization (Fig. 2(a)) is in line with expectation, decreasing with the Vanadium content. The magnetization falls on the Slater-Pauling curve $\mu_0 M_S = 2.2 - 3x$ till $x \approx 40\%$. For larger V content, the magnetization falls off faster, and the sample is paramagnetic at room temperature for $x = 60\%$. The magnetizations for $x \geq 40\%$ are thus influenced by the proximity of Curie temperature T_C and room temperature. The cubic anisotropy field (Fig. 2(b)) also decreases with the Vanadium content, at a rate faster than the magnetization. It changes sign for about 40% of Vanadium and more, and we shall see that the sample properties get less uniform for these compositions.

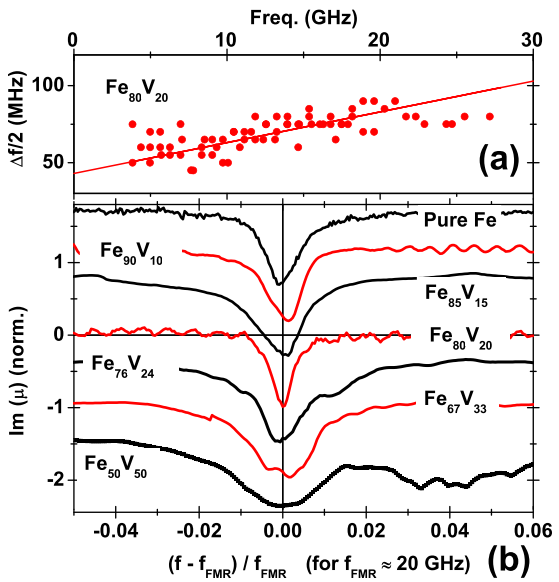

FIG. 3. (a) Half linewidth versus resonance frequency for a $Fe_{80}V_{20}$ film with 18 nm thickness. The line is a linear fit of slope 0.002 and zero frequency intercept 43 MHz. (b) Imaginary part of the permeabilities of 18–20 nm thick FeV alloys for field conditions leading to a resonance frequency near 20 GHz. The curves are vertically offset for clarity. Their amplitude was normalized to unity. The ripple in some spectra is an experimental artifact. The resonance lines have relative half width at half maximum $\Delta\omega/(2\omega)$ listed in Table I. For the sole $x=50\%$ composition, we observed two resonance lines.

TABLE I. Magnetic properties extracted from VNAFMR and PMOKE measurements on MgO (substrate)/FeV (20 nm)/Au (6 nm) films, and comparison with iron literature values and values of films MgO (substrate)/FeV (30 nm)/Ru (3 nm)/Pt (4 nm) deposited by sputtering († symbol). In the damping column, the stars (*) indicate the cases where a substantial inhomogeneous broadening prevents the estimation of the damping. The - symbols recall the samples for which that the PSSW mode could not be detected.

Composition	$\mu_0 M_S$ (T)±0.03	$\mu_0 H_{kc}$ (mT)±2	α_{max} ±10%	$\sqrt{\frac{2A}{\mu_0 M_S^2}}$ (nm)	A (pJ/m)±2
Fe/MgO	2.2	56	≤ 0.0047	3.5	23
$Fe_{90}V_{10}$	1.93	52	≤ 0.0055	4	22
$Fe_{85}V_{15}$	1.72	45	≤ 0.007	4.6	26
$Fe_{80}V_{20}$	1.62	40	≤ 0.0026	4.7	23
$Fe_{76}V_{24}$	1.45	32	≤ 0.006	5.0	22
$Fe_{75}V_{25}$ †	1.25	30	≤ 0.011(*)	6.7	26
$Fe_{67}V_{33}$	1.2	19	≤ 0.008	5.9	24
$Fe_{58}V_{42}$	0.7	−9	≤ 0.028(*)	7.2	10
$Fe_{50}V_{50}$	0.38	−5	≤ 0.01(*)	–	–
$Fe_{40}V_{60}$	0				
Bulk Fe	2.2	55	0.0019 (Ref. 13)	3.2	20.0 (Ref. 35)

More surprising is the dependence of the exchange stiffnesses of the alloys (Table I). Indeed, the exchange stiffness is essentially independent of the Vanadium content as long as $T_C \gg 300$K, i.e., for $x \leq 40\%$. This is opposite to common thinking that would bet on a reduction of the exchange stiffness with the dilution of Fe by the nonmagnetic V. This rather constant A has important consequences: a qualitative estimate of the average exchange integral in a material of given fixed structure (bcc here) is provided by the exchange length. In Table I, we can observe a very clear increase of the exchange length with the Vanadium content. To some extent, this is consistent with the increase of Curie temperature observed[21] in FeV alloys for V contents up to $x \approx 20\%$. This increase in exchange length is technically interesting in storage applications, as it hinders domain wall based reversal that reduce the thermal stability of the magnetization.[8]

The last important parameter is the damping parameter. In most of our samples, the Gilbert damping is so low that the FMR resonance lines include inevitably some inhomogeneous broadening that is difficult to separate from the Gilbert damping contribution. Also for such low damping values, the contributions of Eddy currents are known not to be negligible in our range of thicknesses[30] especially for single-crystalline films like ours. We thus report (Table I) only upper bounds of the Gilbert damping, by saturating the magnetization in the perpendicular direction and using $\alpha_{max} = \Delta\omega/(2\omega_{FMR})$. Star symbols indicate when the frequency dependence of $\Delta\omega/(2\omega_{FMR})$ is indicative of substantial inhomogeneous

broadening. While the damping values are tarnished with some uncertainty, they prove that the damping of FeV alloys can be substantially below that of CoFeB alloys[6] which never fall below 0.004 even for large thicknesses.[26,31,32] We illustrate these exceptionally narrow linewidths in Figure 3(b), where we have gathered the imaginary parts of the permeabilities of our 20 nm thick layers for saturating H_z fields leading to resonances in the vicinity of 20 GHz. There is a marked linewidth minimum for the $Fe_{80}V_{20}$ alloy. Note that this composition is far from $x_V = 64\%$ the composition that would lead to a perfect lattice match between MgO [110] and FeV [100]. Our effective damping record of 0.0026 for 20% of V may thus still be affected by the likely presence of crystal dislocations, such that reducing the lateral dimensions and the thickness may lead to even smaller FMR linewidth at the device level. The reason why this minimum occurs for this specific composition is still to be understood, but may be related to an optimal tradeoff between alloy disorder contributions to damping (more dopants, more electron scattering events affecting the damping[33]), and the beneficial substitution of Fe atom by lower spin-orbit V dopants (more Vanadium dopants lead to a decrease of the spin-flip proportion among the electron scattering events).[14,34]

In summary, we have studied the composition dependence of the magnetic properties of FeV alloy. We have used principally vector network analyzer ferromagnetic resonance to measure the magnetization, anisotropy, exchange stiffness, and damping for all the V contents leading to ferromagnetism at room temperature. The very high exchange stiffness (23 pJ/m) and very low effective damping (<0.0026) of the alloy with 20% of V makes it an interesting candidate for spin torque applications, with potential benefit compared to the standard CoFeB system commonly used. The ultralow damping of FeV alloys substantially smaller than CoFe alloys is consistent with the spin-orbit origin of damping, since V atoms have spin-orbit coefficients 60% lower than iron atoms.[15] Alloying with even lighter elements like Ti may thus be a way to further reduce the damping provided the crystalline quality of the material can be maintained. This work was supported by the PPF SPINEL program of the "Université Paris-Sud."

[1]T. Min, Q. Chen, R. Beach, G. Jan, C. Horng, W. Kula, T. Torng, R. Tong, T. Zhong, D. Tang, P. Wang, M. Chen, J. Sun, J. Debrosse, D. Worledge, T. Maffitt, and W. Gallagher, IEEE Trans. Magn. **46**, 2322 (2010).
[2]A. V. Khvalkovskiy, D. Apalkov, S. Watts, R. Chepulskii, R. S. Beach, A. Ong, X. Tang, A. Driskill-Smith, W. H. Butler, P. B. Visscher, D. Lottis, E. Chen, V. Nikitin, and M. Krounbi, J. Phys. D: Appl. Phys. **46**, 074001 (2013).
[3]S. Ikeda, K. Miura, H. Yamamoto, K. Mizunuma, H. D. Gan, M. Endo, S. Kanai, J. Hayakawa, F. Matsukura, and H. Ohno, Nature Mater. **9**, 721 (2010).
[4]Y. M. Lee, J. Hayakawa, S. Ikeda, F. Matsukura, and H. Ohno, Appl. Phys. Lett. **90**, 212507 (2007).
[5]T. Devolder, J. Hayakawa, K. Ito, H. Takahashi, S. Ikeda, P. Crozat, N. Zerounian, J.-V. Kim, C. Chappert, and H. Ohno, Phys. Rev. Lett. **100**, 057206 (2008).
[6]T. Devolder, P.-H. Ducrot, J.-P. Adam, I. Barisic, N. Vernier, J.-V. Kim, B. Ockert, and D. Ravelosona, Appl. Phys. Lett. **102**, 022407 (2013).
[7]T. Devolder, I. Barisic, S. Eimer, K. Garcia, J.-P. Adam, B. Ockert, and D. Ravelosona, J. App. Phys. **113**, 203912 (2013).
[8]J. Z. Sun, R. P. Robertazzi, J. Nowak, P. L. Trouilloud, G. Hu, D. W. Abraham, M. C. Gaidis, S. L. Brown, E. J. O'Sullivan, W. J. Gallagher, and D. C. Worledge, Phys. Rev. B **84**, 064413 (2011).
[9]S. M. Bhagat and P. Lubitz, Phys. Rev. B **10**, 179 (1974).
[10]H. Kubota, A. Fukushima, K. Yakushiji, S. Yakata, S. Yuasa, K. Ando, M. Ogane, Y. Ando, and T. Miyazaki, J. Appl. Phys. **105**, 07D117 (2009).
[11]K. Oguz, M. Ozdemir, O. Dur, and J. M. D. Coey, J. Appl. Phys. **111**, 113904 (2012).
[12]P. He, X. Ma, J. W. Zhang, H. B. Zhao, G. Lüpke, Z. Shi, and S. M. Zhou, Phys. Rev. Lett. **110**, 077203 (2013).
[13]C. Scheck, L. Cheng, I. Barsukov, Z. Frait, and W. E. Bailey, Phys. Rev. Lett. **98**, 117601 (2007).
[14]V. Kambersky, Czech. J. Phys. B **26**, 1366 (1976).
[15]E. Francisco and L. Pueyo, Phys. Rev. A **36**, 1978 (1987).
[16]A. R. Mackintosh and O. K. Andersen, in *Electrons at the Fermi Surface*, edited by M. Springford (Cambridge University Press, 2011).
[17]M. Sicot, S. Andrieu, F. Bertran, and F. Fortuna, Phys. Rev. B **72**, 144414 (2005).
[18]H. V. Elst, B. Lubach, and G. V. den Berg, Physica **28**, 1297 (1962).
[19]K. Fukamichi, H. Hiroyoshi, T. Kaneko, T. Masumoto, and K. Shirakawa, J. Appl. Phys. **53**, 8107 (1982).
[20]Y. Kakehashi, Phys. Rev. B **32**, 3035 (1985).
[21]R. M. Bozorth, *Ferromagnetism* (IEEE Inc., New York, 1993).
[22]F. Bonell, S. Andrieu, F. Bertran, P. Lefevre, A. T. Ibrahimi, E. Snoeck, C.-V. Tiusan, and F. Montaigne, IEEE Trans. Magn. **45**, 3467 (2009).
[23]F. Bonell, S. Andrieu, C. Tiusan, F. Montaigne, E. Snoeck, B. Belhadji, L. Calmels, F. Bertran, P. Le Fèvre, and A. Taleb-Ibrahimi, Phys. Rev. B **82**, 092405 (2010).
[24]C.-H. Lambert, A. Rajanikanth, T. Hauet, S. Mangin, E. E. Fullerton, and S. Andrieu, Appl. Phys. Lett. **102**, 122410 (2013).
[25]A. Rajanikanth, T. Hauet, F. Montaigne, S. Mangin, and S. Andrieu, Appl. Phys. Lett. **103**, 062402 (2013).
[26]C. Bilzer, T. Devolder, J.-V. Kim, G. Counil, C. Chappert, S. Cardoso, and P. P. Freitas, J. Appl. Phys. **100**, 053903 (2006).
[27]C. Bilzer, T. Devolder, P. Crozat, and C. Chappert, IEEE Trans. Magn. **44**, 3265 (2008).
[28]M. Bailleul, in *ICMM 2012 Conference*, 2012.
[29]R. D. McMichael, M. D. Stiles, P. J. Chen, and J. W. F. Egelhoff, J. Appl. Phys. **83**, 7037 (1998).
[30]B. Heinrich, in *Ultrathin Magnetic Structures III*, edited by J. A. C. Bland and B. Heinrich (Springer, 2005).
[31]A. Conca, J. Greser, T. Sebastian, S. Klingler, B. Obry, B. Leven, and B. Hillebrands, J. Appl. Phys. **113**, 213909 (2013).
[32]X. Liu, W. Zhang, M. J. Carter, and G. Xiao, J. Appl. Phys. **110**, 033910 (2011).
[33]G. Counil, T. Devolder, J.-V. Kim, P. Crozat, C. Chappert, S. Zoll, and R. Fournel, IEEE Trans. Magn. **42**, 3323 (2006).
[34]J. O. Rantschler, R. D. McMichael, A. Castillo, A. J. Shapiro, J. W. F. Egelhoff, B. B. Maranville, D. Pulugurtha, A. P. Chen, and L. M. Connors, J. Appl. Phys. **101**, 033911 (2007).
[35]J. F. Cochran, "Light scattering from ultrathin magnetic layers and bilayers," in *Ultrathin Magnetic Structures II*, edited by B. Heinrich and J. A. C. Bland (Springer, 1994).